# DRUG PARTICLES SMALLER THAN EVER BEFORE



40 µm

**BEFORE NANOFORMING™**

**AFTER NANOFORMING™**

5 µm

## Working with you to enhance drug effectiveness and targeting

Our global experts in nanotechnology and drug particle engineering can help your drugs reach their full therapeutic potential. With the unique ability to produce nanoparticles as small as 10 nm, our award-winning Controlled Expansion of Supercritical Solutions (CESS®) technology can increase dissolution rates and improve bioavailability. Together, we can initiate a new era of novel drug development and enable more patients around the world to benefit from next-generation drug therapies.

**nanoform**
small is powerful

Contact Nanoform to unlock the potential of your molecules +358 29 370 0150

nanoform.com  |  info@nanoform.com

@NanoformF    in Nanoform

DDR

# Research Article

# Synthesis of Five- and Six-Membered *N*-Phenylacetamido Substituted Heterocycles as Formyl Peptide Receptor Agonists

Claudia Vergelli,[1] Igor A. Schepetkin,[2] Giovanna Ciciani,[1] Agostino Cilibrizzi,[3] Letizia Crocetti,[1] Maria Paola Giovannoni,[1]* Gabriella Guerrini,[1] Antonella Iacovone,[1] Liliya N. Kirpotina,[2] Richard D. Ye,[4] and Mark T. Quinn[2]

[1]*Department of NEUROFARBA, Sezione di Farmaceutica e Nutraceutica, Università degli Studi di Firenze, Via Ugo Schiff 6, Sesto, Fiorentino 50019, Italy*
[2]*Department of Microbiology and Immunology, Montana State University, Bozeman, Montana 59717*
[3]*Department of Chemistry, Imperial College London, South Kensington, London SW7 2AZ, United Kingdom*
[4]*Institute of Chinese Medical Sciences, University of Macau, Macau, China*

| Strategy, Management and Health Policy | | | | |
|---|---|---|---|---|
| Enabling Technology, Genomics, Proteomics | Preclinical Research | Preclinical Development Toxicology, Formulation Drug Delivery, Pharmacokinetics | Clinical Development Phases I-III Regulatory, Quality, Manufacturing | Postmarketing Phase IV |

**ABSTRACT**      Formyl peptide receptors (FPRs) are G-protein-coupled receptors that play an important role in the regulation of inflammatory process and cellular dysfunction. In humans, three different isoforms are expressed (FPR1, FPR2, and FPR3). FPR2 appears to be directly involved in the resolution of inflammation, an active process carried out by specific pro-resolving mediators that modulate specific receptors. Previously, we identified 2-arylacetamido pyridazin-3(2*H*)-ones as FPR1- or FPR2-selective agonists, as well as a large number of mixed-agonists for the three isoforms. Here, we report a new series of 2-arylacetamido pyridazinones substituted at position 5 and their development as FPR agonists. We also synthesized a new series of 2-oxothiazolones bearing a 4-bromophenylacetamido fragment, which was fundamental for activity in the pyridazinone series. The compounds of most interest were **4a**, a potent, mixed FPR agonist recognized by all three isotypes (FPR1 $EC_{50} = 19$ nM, FPR2 $EC_{50} = 43$ nM, FPR3 $EC_{50} = 40$ nM), and **4b**, which had potent activity and a preference for FPR2 ($EC_{50} = 13$ nM). These novel compounds may represent valuable tools for studying FPR activation and signaling. Drug Dev Res 78 : 49–62, 2017.      © 2016 Wiley Periodicals, Inc.

Key words: formyl peptide receptor; agonist; pyridazin-3(2H)-one; neutrophil; Ca2+ flux

## INTRODUCTION

Inflammation is a primary response of the immune system to injury or infection by invading microbial pathogens and is mediated by the action of many cell types with distinct functions [Beutler, 2004]. The critical role of the inflammatory process in health and disease is essential; however, the mechanisms leading to the restoration of homeostasis and resolution of inflammation (ROI) have only recently been elucidated. These studies have demonstrated that the ROI is an active process carried out by specific pro-resolving mediators, such as lipoxin, resolvins, protectins, and maresins, which have anti-inflammatory and pro-resolving activities that are mediated via interactions with specific receptors [Serhan et al., 2002; Serhan and Levy, 2003; Serhan et al., 2011; Serhan et al., 2015]. Among the receptors activated by pro-resolving mediators is formyl peptide receptor 2 (FPR2), which belongs to a group of G-protein coupled receptors [Corminboeuf and Leroy, 2015]. In addition to FPR2, two other isoforms, FPR1 and FPR3, have been identified in humans and exhibit a high level of amino acid homology with FPR2 [Ye et al., 2009]. Despite their high level of sequence homology, the FPRs differ in their ability to bind the prototypic $N$-formyl peptide $N$-formyl-methionine-leucine-phenylalanine ($f$MLF). FPR1 has high affinity receptor for this ligand, FPR2 low-affinity receptor, while FPR3 does not bind $f$MLF. FPR1 and FPR2 have a similar distribution in a variety of tissues and cells involved in inflammation, including endothelial cells, platelets and immature dendritic cells, monocytes, neutrophils, macrophages, T lymphocytes, and epithelial cells [Migeotte et al., 2006; Ye et al., 2009], whereas FPR3 is expressed in monocytes and dendritic cells [Migeotte et al., 2005, 2006].

The involvement of FPR2 in the ROI makes this receptor an attractive target for treating a variety of pathologies, including rheumatoid arthritis, asthma, chronic obstructive pulmonary disease, cancer, cardiovascular, and Alzheimer's diseases [Libby, 2002, 2015; Mantovani et al., 2008; Bozinovski et al., 2013]. There are only a few reported examples of FPR2-selective ligands [Schepetkin et al., 2014a].

Our research in the field of FPR ligands led to the identification of a large number of pyridazin-3(2$H$)-one derivatives that were mixed FPR1/FPR2 agonists (Fig. 1, general structure A) [Cilibrizzi et al., 2009, 2012; Cilibrizzi et al., 2013; Crocetti et al., 2013; Giovannoni et al., 2013, Vergelli et al., 2016]. Key requirements for activity were the presence of a methyl group at position 6 of the pyridazinone ring, a
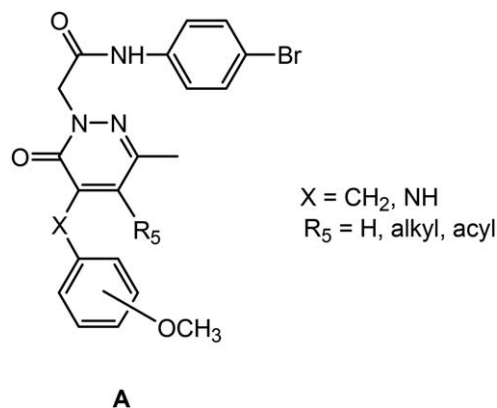


**Fig. 1.** FPR1/FPR2 mixed agonists.

4-bromophenylacetamide moiety at $N$-2, and a benzyl/aniline group at position 4 of the scaffold. In the series of 4-anilino derivatives, we identified some compounds with good potency and with a moderate preference for FPR2 subtype [Vergelli et al., 2016]. In the present article, we further investigated 4-benzylpyridazinones derivatives as isosteres of the 4-anilino derivatives and examine their structure-activity relationships [Vergelli et al., 2016], as well as several derivatives lacking a benzyl fragment at position 4. We also synthesized and evaluated a series of 2-oxothiazolones by maintaining the 4-bromophenylacetamide side fragment.

## MATERIALS AND METHODS
### Chemistry

The synthetic pathways followed to obtain the final compounds are shown in Figures 2 and 3, and the structures were confirmed by analytical and spectral data.

In Figure 2, synthesis of the 4-benzylpyridazinones **4a-f** and the 4-unsubstituted derivatives of type **6** and **7** is presented. Previously described oxoacids **1a-e** [Metz and Schwenker, 1980; Xu et al., 2005; Holloway et al., 2010] were reacted with hydrazine hydrate to obtain the corresponding 4,5-dihydropyridazinones (±)**2a-e** (compounds (±)**2a,b,d** [Pinna et al., 1988; Haider and Holzer, 2004; Xu et al., 2005]), which were converted into derivatives **3a-f** by treatment with the appropriate arylaldehyde in the presence of KOH. Alkylation of **3a-f** with commercially available $N$-(4-bromophenyl)−2-chloroacetamide in anhydrous $CH_3CN$ resulted in the final compounds **4a-f**. Compounds (±)**2a,b** [Pinna et al., 1988; Haider and Holzer, 2004] were also key intermediates for the synthesis of 4-unsubstituted derivatives **6** and **7** by direct alkylation with $N$-(4-bromophenyl)−2-chloroacetamide (compounds **6a,b**) or
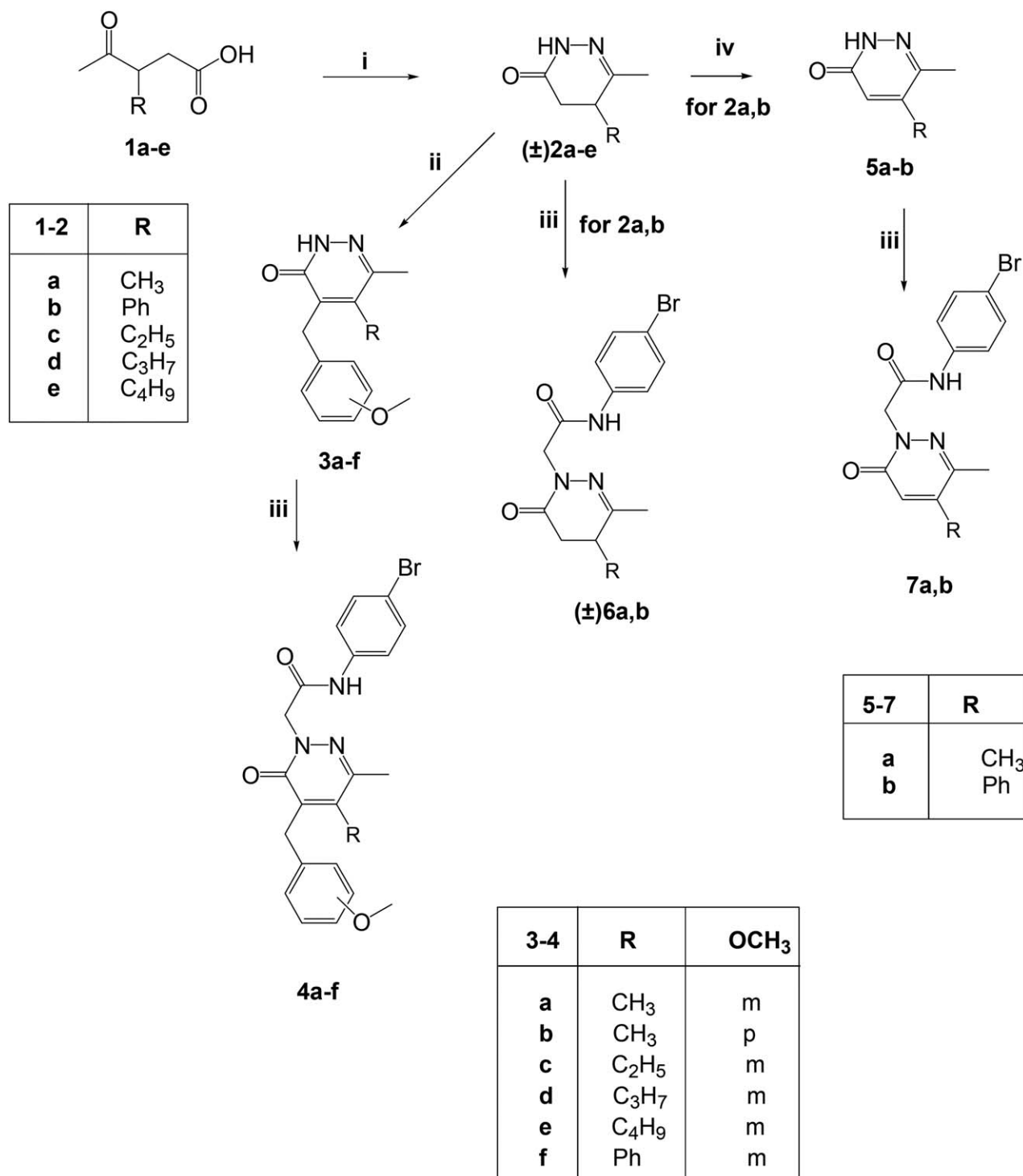
**Fig. 2.** Synthesis of the final compounds **4a-f**, (±)**6a,b**, **7a,b**. Reagents and conditions: (i) $N_2H_4$ $H_2O$, EtOH, reflux, 3h; (ii) 3 or 4-methoxybenzaldehyde, KOH 5% (w/v) in anhydrous EtOH, reflux, 7–20 h; (iii) N-(4-bromophenyl)-2-chloroacetamide, $K_2CO_3$, anhydrous $CH_3CN$, reflux, 5–7 h; (iv) $Br_2$/AcOH, reflux, 8h.

by oxidation with $Br_2$ and acetic acid (compounds **5a,b**) [Coates and McKillop, 1993; Haider and Holzer, 2004] and further alkylation (**7a,b**).

In Figure 3, synthesis of the final oxothiazolones **9a-h** and **10** is presented. The previously described compounds **8a-h** [Isomura et al., 1988; Pihlaja et al.,
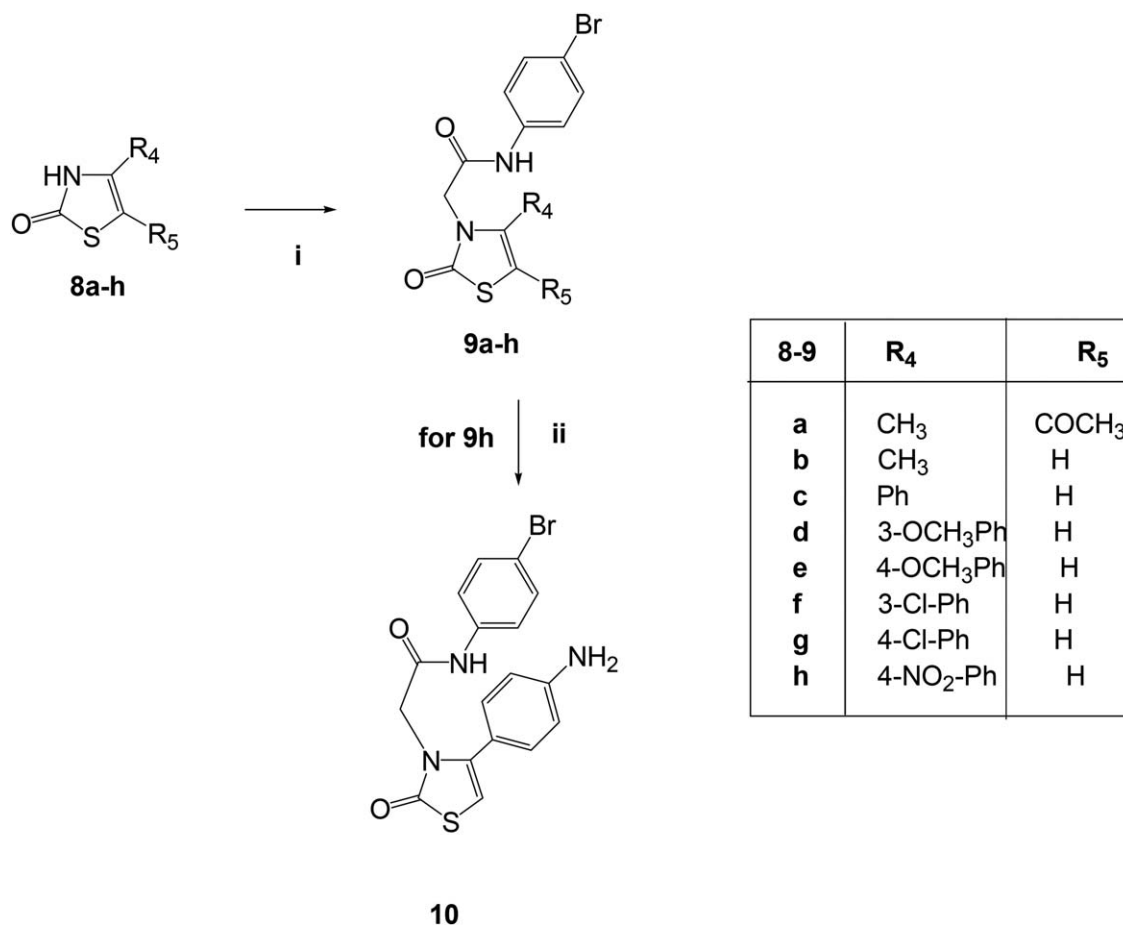
**Fig. 3.** Synthesis of the final compounds **9a-h** and **10**. Reagents and conditions: (i) *N*-(4-bromophenyl)-2- chloroacetamide, K$_2$CO$_3$,anhydrou CH$_3$CN, reflux, 5–7 h; (ii) 10% Pd/C, anhydrous EtOH, H$_2$, Parr, 30 PSI, 2 h.

2002; Wang et al., 2005; Yarligan et al., 2005; Zhao et al., 2013] were alkylated as shown to obtain the desired **9a-h**. The final **9h** was then subject to catalytic reduction with Pd/C in a Parr instrument to obtain compound **10**.

### Experimentals

Reagents and starting materials were obtained from commercial sources. Extracts were dried over Na$_2$SO$_4$, and the solvents were removed under reduced pressure. All reactions were monitored by thin layer chromatography (TLC) using commercial plates pre-coated with Merck silica gel 60 F-254, and visualization was performed by UV fluorescence ($\lambda_{max} = 254$ nm) or by staining with iodine or potassium permanganate. Chromatographic separations were performed on a silica gel column using gravity chromatography (Kieselgel 40, 0.063–0.200 mm; Merck), flash chromatography (Kieselgel 40, 0.040–0.063 mm; Merck), or silica gel preparative TLC (Kieselgel 60 F$_{254}$, 20 × 20 cm, 2 mm). Yields refer to chromatographically and spectroscopically pure compounds, unless otherwise stated. Compounds are named following IUPAC rules, as applied by Beilstein-Institut AutoNom 2000 (4.01.305) or CA Index Name. All melting points were determined on a microscope hot stage Büchi apparatus and are uncorrected. The identity and purity of intermediates and final compounds were determined through NMR analysis and TLC chromatography. $^{1}$H NMR, $^{13}$C NMR and NOESY spectra were recorded with Avance 400 instruments (Bruker Biospin Version 002 with SGU). Chemical shifts ($\delta$) are reported in ppm to the nearest 0.01 ppm (for $^{1}$H NMR) or 0.1 ppm (for $^{13}$C NMR) using the solvent as an internal standard. Coupling constants (*J* values) of $^{1}$H NMR are given in Hz and were calculated using "TopSpin 1.3" software and rounded to the nearest 0.1 Hz. Microanalyses were performed with a Perkin-Elmer 260 elemental analyzer for C, H, and N, and the results were within ± 0.4% of the theoretical values, unless otherwise stated.

## General Procedures for (±)2c and (±)2e

To a solution of appropriate acid **1c** and **1e** (1.52 mmol) [Holloway et al., 2010] in EtOH (5 mL), hydrazine hydrate (3.04 mmol) was added. The mixture was refluxed for 3 h. After cooling, the solvent was evaporated under vacuum and cold water (10 mL) was added. The suspension was extracted with $CH_2Cl_2$ (3 × 15 mL), the organic phase was dried over $Na_2SO_4$ and evaporated to give the final compounds (±)**2c** and (±)**2e**.

## (±)5-Ethyl-6-Methyl-4,5-Dihydropyridazin-3(2H)-One, (±)2c

Yield = 26%; oil. $^1$H-NMR (CDCl$_3$) $\delta$ 0.94 (t, 3H, $CH_3$CH$_2$, J = 7.2 Hz); 1.50–1.65 (m, 2H, CH$_2$CO); 2.00 (s, 3H, CH$_3$C = N); 2.30–2.38 (m, 2H, CH$_3$$CH_2$); 2.47–2.53 (m, 1H, $CH$CH$_2$CH$_3$); 9.17 (exch br s, 1H, NH). Anal. Calcd for $C_7H_{12}N_2O$ (140.18): C, 59.98; H, 8.63; N, 19.98; Found: C, 59.85; H, 8.65; N, 19.92.

## (±)5-Butyl-6-Methyl-4,5-Dihydropyridazin-3(2H)-One, (±)2e

Yield = 34%; mp = 63–67°C (Cyclohexane). $^1$H-NMR (CDCl$_3$) $\delta$ 0.91–0.95 (m, 3H, $CH_3$(CH$_2$)$_3$); 1.32–1.37 (m, 2H, CH$_3$$CH_2$(CH$_2$)$_2$); 1.44–1.50 (m, 2H, CH$_3$CH$_2$$CH_2$CH$_2$); 1.87–1.89 (m, 2H, CH$_3$(CH$_2$)$_2$$CH_2$); 2.07 (s, 3H, CH$_3$C = N); 2.37–2.42 (m, 1H, $CH$(CH$_2$)$_3$CH$_3$); 2.48–2.60 (m, 2H, CH$_2$CO); 8.24 (exch br s, 1H, NH). Anal. Calcd for $C_9H_{16}N_2O$ (168.24): C, 64.25; H, 9.59; N, 16.65; Found: C, 64.41; H, 9.58; N, 16.59.

## General Procedures for 3a-f

To a solution of the suitable intermediate (±)**2a-e** ((±)**2a,b** and (±)**2d** [Pinna et al., 1988; Haider and Holzer, 2004; Xu et al., 2005]) (1.44 mmol) in 5–9 mL of KOH/absolute EtOH (5% w/v), 3- or 4-methoxybenzaldehyde (1.44–2.16 mmol) was added and the mixture was refluxed under stirring for 7–20 h. After cooling, the mixture was concentrated *in vacuo*, diluted with ice-cold water (5–10 mL), neutralized with N HCl and extracted with $CH_2Cl_2$ (3 ×x 20 mL). Removal of the solvent resulted in crude compounds **3a,b,f**, which were purified by flash chromatography using cyclohexane/ethyl acetate 1:3 (for **3a,b**) and cyclohexane/ethyl acetate 2:1 (for **3f**) as eluents. Compounds **3c-e** were recovered as crude precipitate after dilution and neutralization. These final compounds were purified by crystallization from EtOH.

## 4-(3-methoxybenzyl)-5,6-Dimethylpyridazin-3(2H)-One, 3a

Yield = 58%; mp = 185–186°C (EtOH). $^1$H-NMR (CDCl$_3$) $\delta$ 2.18 (s, 3H, N = C$CH_3$); 2.28 (s, 3H, CH$_3$); 3.79 (s, 3H, OCH$_3$); 4.03 (s, 2H, CH$_2$); 6.76 (d, 1H, Ar, J = 10.8 Hz); 6.81–6.83 (m, 2H, Ar); 7.20 (t, 1H, Ar, J = 8.0 Hz); 9.98 (exch br s, 1H, NH). Anal. Calcd for $C_{14}H_{16}N_2O_2$ (244.29): C, 68.83; H, 6.60; N, 11.47; Found: C, 69.01; H, 6.59; N, 11.50.

## 4-(4-methoxybenzyl)-5,6-Dimethylpyridazin-3(2H)-One, 3b

Yield = 44%; mp = 150–151°C (EtOH). $^1$H-NMR (CDCl$_3$) $\delta$ 2.19 (s, 3H, N = C$CH_3$); 2.28 (s, 3H, CH$_3$); 3.79 (s, 3H, OCH$_3$); 3.98 (s, 2H, CH$_2$); 6.82 (d, 2H, Ar, J = 8.4 Hz); 7.21 (d, 2H, Ar, J = 8.4 Hz); 10.33 (exch br s, 1H, NH). Anal. Calcd for $C_{14}H_{16}N_2O_2$ (244.29): C, 68.83; H, 6.60; N, 11.47; Found: C, 68.99; H, 6.59; N, 11.49.

## 5-Ethyl-4-(3-methoxybenzyl)-6-Methylpyridazin-3(2H)-One, 3c

Yield = 44%; mp = 168–170°C (EtOH). $^1$H-NMR (CDCl$_3$) $\delta$ 1.08 (t, 3H, $CH_3$CH$_2$, J = 7.6 Hz); 2.37 (s, 3H, N = C$CH_3$); 2.62 (q, 2H, CH$_3$$CH_2$, J = 7.6 Hz); 3.79 (s, 3H, OCH$_3$); 4.03 (s, 2H, $CH_2$Ph); 6.76 (m, 1H, Ar); 6.82 (m, 2H, Ar); 7.20 (m, 1H, Ar). Anal. Calcd for $C_{15}H_{18}N_2O_2$ (258.32): C, 69.74; H, 7.02; N, 10.84; Found: C, 69.91; H, 7.01; N, 10.87.

## 4-(3-methoxybenzyl)-6-Methyl-5-Propylpyridazin-3(2H)-One, 3d

Yield = 23%; mp = 134–137°C (EtOH). $^1$H-NMR (CDCl$_3$) $\delta$ 1.00 (t, 3H, $CH_3$(CH$_2$)$_2$, J = 7.6 Hz); 1.38–1.44 (m, 2H, CH$_3$$CH_2$CH$_2$); 2.33 (s, 3H, N = C$CH_3$); 2.49–2.54 (m, 2H, CH$_3$CH$_2$$CH_2$); 3.79 (s, 3H, OCH$_3$); 4.03 (s, 2H, $CH_2$Ph); 6.75 (m, 1H, Ar); 6.82–6.85 (m, 2H, Ar); 7.19 (t, 1H, Ar, J = 7.2 Hz). Anal. Calcd for $C_{16}H_{20}N_2O_2$ (272.34): C, 70.56; H, 7.40; N, 10.29; Found: C, 70.39; H, 7.41; N, 10.23.

## 5-Butyl-4-(3-methoxybenzyl)-6-Methylpyridazin-3(2H)-One, 3e

Yield = 22%; mp = 144–146°C (EtOH/H$_2$O 1:1). $^1$H-NMR (CDCl$_3$) $\delta$ 0.95 (t, 3H, $CH_3$(CH$_2$)$_3$, J = 7.2 Hz); 1.32–1.46 (m, 4H, CH$_3$$CH_2$CH$_2$CH$_2$); 2.35 (s, 3H, N = C$CH_3$); 2.52–2.57 (m, 2H, CH$_3$CH$_2$CH$_2$$CH_2$); 3.79 (s, 3H, OCH$_3$); 4.02 (s, 2H, $CH_2$Ph); 6.76 (m, 1H, Ar); 6.82 (m, 2H, Ar); 7.19 (t, 1H, Ar, J = 7.6 Hz). Anal.

Calcd for $C_{17}H_{22}N_2O_2$ (286.37): C, 71.30; H, 7.74; N, 9.78; Found: C, 71.49; H, 7.75; N, 9.81.

### 4-(3-methoxybenzyl)-6-Methyl-5-Phenylpyridazin-3(2*H*)-One, 3f

Yield = 32%; oil. $^1$H-NMR (CDCl$_3$) $\delta$ 2.14 (s, 3H, N = CCH$_3$); 3.73 (s, 3H, OCH$_3$); 3.80 (s, 2H, CH$_2$); 6.42 (s, 1H, Ar); 6.53 (d, 1H, Ar, J = 10.8 Hz); 6.71 (dd, 1H, Ar, J = 2.4 Hz, J = 5.6 Hz); 7.02–7.17 (m, 3H, Ar); 7.41–7.51 (m, 3H, Ar). Anal. Calcd for $C_{19}H_{18}N_2O_2$ (306.36): C, 74.49; H, 5.92; N, 9.14; Found: C,74.68; H, 5.91; N, 9.16.

### General Procedures for 4a-f

To a mixture of the appropriate intermediate **3a-f** (0.40 mmol) and K$_2$CO$_3$ (0.80–1.20 mmol) in CH$_3$CN (5–10 mL), *N*-(4-bromophenyl)−2-chloroacetamide (0.40–0.72 mmol) was added and the suspension was refluxed under stirring for 5–7 h. After cooling, the mixture was concentrated *in vacuo*, ice cold water was (5–10 mL) added and then further stirred for 1 h. The precipitate was recovered by suction and purified by flash chromatography using cyclohexane/ethyl acetate 1:1 (compounds **4a,b,e**), cyclohexane/ethyl acetate 1:2 (compounds **4c,d**) and cyclohexane/ethyl acetate 2:1 for **4f** as eluents.

### N-(4-bromophenyl)-2-[5-(3-methoxybenzyl)-3,4-dimethyl-6-oxopyridazin-1(6H)-Yl]Acetamide, 4a

Yield = 48%; mp = 123–124°C (EtOH). $^1$H-NMR (CDCl$_3$) $\delta$ 2.23 (s, 3H, N = CCH$_3$); 2.34 (s, 3H, C = CCH$_3$); 3.76 (s, 3H, OCH$_3$); 4.06 (s, 2H, CH$_2$Ar); 4.94 (s, 2H, NCH$_2$); 6.76 (dd, 1H, Ar, J = 6.4 Hz, J = 1.6 Hz); 6.79–6.82 (m, 2H, Ar); 7.19 (t, 1H, Ar, J = 8.0 Hz); 7.30–7.35 (m, 4H, Ar); 9.31 (exch br s, 1H, NH). $^{13}$C-NMR (CDCl$_3$) $\delta$ 16.0 (**CH$_3$**); 20.4 (CH$_3$); 32.1 (CH$_2$); 55.1 (CH$_3$); 57.9 (CH$_2$); 111.3 (CH); 114.7 (CH); 116.3 (C); 120.7 (CH); 121.1 (2 CH); 129.5 (CH); 131.5 (2CH); 137.1 (C); 137.9 (C); 139.4 (C); 140.7 (C); 146.6 (C); 159.8 (C); 161.2 (C); 165.6 (C). Anal. Calcd for $C_{22}H_{22}N_3O_3$ (456.33): C, 57.90; H, 4.86; N, 9.21; Found: C, 57.74; H, 4.85; N, 9.24.

### N-(4-bromophenyl)-2-[5-(4-methoxybenzyl)-3,4-dimethyl-6-oxopyridazin-1(6H)-Yl]Acetamide, 4b

Yield = 58%; mp = 177–178°C (EtOH). $^1$H-NMR (CDCl$_3$) $\delta$ 2.24 (s, 3H, N = CCH$_3$); 2.33 (s, 3H, C = CCH$_3$); 3.78 (s, 3H, OCH$_3$); 4.02 (s, 2H, CH$_2$Ar); 4.94 (s, 2H, NCH$_2$); 6.80 (d, 2H, Ar, J = 8.4 Hz); 7.16 (d, 2H, Ar, J = 8.4 Hz); 7.30–7.38 (m, 4H, Ar); 9.26 (exch br s, 1H, NH). $^{13}$C-NMR (CDCl$_3$) $\delta$ 16.0 (CH$_3$); 20.3 (CH$_3$); 31.3 (CH$_2$); 55.2 (CH$_3$); 58.1 (CH$_2$); 114.1 (2 CH); 116.4 (C); 121.2 (2CH); 129.4 (2 CH); 129.6 (C); 131.5 (2 CH); 137.0 (C); 138.5 (C); 140.3 (C); 146.8 (C); 158.3 (C); 161.2 (C); 165.6 (C). Anal. Calcd for $C_{22}H_{22}N_3O_3$ (456.33): C, 57.90; H, 4.86; N, 9.21; Found: C, 57.69; H, 4.85; N, 9.18.

### N-(4-bromophenyl)-2-[4-ethyl-5-(3-methoxybenzyl)-3-methyl-6-oxopyridazin-1(6H)-Yl]Acetamide, 4c

Yield = 39%; mp = 86–88°C (EtOH). $^1$H-NMR (CDCl$_3$) $\delta$ 1.10 (t, 3H, *CH$_3$*CH$_2$, J = 7.6 Hz); 2.39 (s, 3H, N = CCH$_3$); 2.63 (q, 2H, CH$_3$*CH$_2$*, J = 7.6 Hz); 3.75 (s, 3H, OCH$_3$); 4.05 (s, 2H, *CH$_2$*Ar); 4.93 (s, 2H, *CH$_2$*CO); 6.77 (m, 3H, Ar); 7.18 (t, 1H, Ar, J = 8.8 Hz); 7.33–7.38 (m, 4H, Ar); 9.31 (exch br s, 1H, NH). Anal. Calcd for $C_{23}H_{24}BrN_3O_3$ (470.36): C, 58.73; H, 5.14; N, 8.93; Found: C, 58.89; H, 5.13; N, 8.90.

### N-(4-bromophenyl)-2-[5-(3-methoxybenzyl)-3-methyl-6-oxo-4-propylpyridazin-1(6H)-yl]Acetamide, 4d

Yield = 30%; mp = 81–83°C (EtOH). $^1$H-NMR (CDCl$_3$) $\delta$ 1.04 (t, 3H, *CH$_3$*(CH$_2$)$_2$, J = 7.2 Hz); 1.42–1.49 (m, 2H, CH$_3$*CH$_2$*CH$_2$); 2.38 (s, 3H, N = CCH$_3$); 2.54–2.58 (m, 2H, CH$_3$CH$_2$*CH$_2$*); 3.74 (s, 3H, OCH$_3$); 4.03 (s, 2H, *CH$_2$*Ar); 4.88 (s, 2H, *CH$_2$*CO); 6.74–6.78 (m, 3H, Ar); 7.17 (t, 1H, Ar, J = 7.6 Hz); 7.25 (m, 4H, Ar); 9.50 (exch br s, 1H, NH). Anal. Calcd for $C_{24}H_{26}BrN_3O_3$ (484.39): C, 59.51; H, 5.41; N, 8.67; Found: C, 59.67; H, 5.40; N, 8.64.

### N-(4-bromophenyl)-2-[4-butyl-5-(3-methoxybenzyl)-3-methyl-6-oxopyridazin-1(6H)-yl]Acetamide, 4e

Yield = 57%; mp = 75–77°C (Cyclohexane). $^1$H-NMR (CDCl$_3$) $\delta$ 0.93 (t, 3H, *CH$_3$*(CH$_2$)$_3$, J = 7.2 Hz); 1.28–1.45 (m, 4H, CH$_3$*CH$_2$CH$_2$*CH$_2$); 2.38 (s, 3H, N = CCH$_3$); 2.54–2.58 (m, 2H, CH$_3$CH$_2$CH$_2$*CH$_2$*); 3.73 (s, 3H, OCH$_3$); 3.99 (s, 2H, *CH$_2$*Ar); 4.88 (s, 2H, *CH$_2$*CO); 6.75–6.78 (m, 3H, Ar); 7.17 (t, 1H, Ar, J = 7.6 Hz). 7.25–7.27 (m, 4H, Ar); 9.53 (exch br s, 1H, NH). Anal. Calcd for $C_{25}H_{28}BrN_3O_3$ (498.41): C, 60.24; H, 5.66; N, 8.43; Found: C, 60.08; H, 5.66; N, 8.46.

### N-(4-bromophenyl)-2-[5-(3-methoxybenzyl)-3-methyl-6-oxo-4-phenylpyridazin-1(6H)-yl]Acetamide, 4f

Yield = 24%; oil. $^1$H-NMR (CDCl$_3$) $\delta$ 2.09 (s, 3H, CCH$_3$,); 3.65 (s, 3H, OCH$_3$); 3.87 (s, 2H, *CH$_2$*Ar); 5.00 (s, 2H, NCH$_2$); 6.38 (s, 1H, Ar); 6.64

(d, 1H, Ar, $J = 8.8$ Hz); 7.02–7.06 (m, 2H, Ar); 7.19 (d, 1H, Ar, $J = 7.6$ Hz); 7.42 (m, 8H, Ar); 9.22 (exch br s, 1H, NH). $^{13}$C-NMR (CDCl$_3$) $\delta$ 21.1 (CH$_3$); 31.1 (CH$_2$); 55.2 (CH$_3$); 58.3 (CH$_2$); 111.4 (CH); 112.1 (CH); 114.7 (CH); 115.3 (CH); 116.4 (C); 120.9 (CH); 121.1 (CH); 125.4 (C); 127.5 (CH); 128.0 (CH); 128.8 (CH); 129.0 (CH); 129.3 (CH); 129.8 (CH); 131.5 (CH); 134.7 (C); 137.0 (C); 138.5 (C); 139.7 (C); 145.2 (C); 145.8 (C); 161.2 (C); 165.5 (C). Anal. Calcd for C$_{27}$H$_{24}$N$_3$O$_3$ (518.40): C, 62.56; H, 4.67; N, 8.11; Found: C, 62.74; H, 4.68; N, 8.13.

### General Procedures for (±)6a,b and 7a,b

Compounds (±)6a,b and 7a,b were obtained starting from appropriate substrates (±)2a,b [Pinna et al., 1988; Haider and Holzer, 2004] and 5a,b [Coates and McKillop, 1993; Haider and Holzer, 2004] following the same procedure described for 4a-f. The final compounds were purified by column chromatography using cyclohexane/ethyl acetate 1:1 as eluent.

### (±)N-(4-bromophenyl)-2-[3,4-dimethyl-6-oxo-5,6-dihydropyridazin-1(4H)-yl]Acetamide, (±)6a

Yield = 36%; mp = 84–85°C (EtOH). $^1$H-NMR (CDCl$_3$) $\delta$ 1.22 (d, 3H, CH*CH$_3$*, $J = 6.8$ Hz); 2.08 (s, 3H, N = CCH$_3$); 2.33–2.40 (m, 1H, CH$_3$*CH*); 2.64–2.70 (m, 2H, CHCH$_2$); 4.49 (d, 1H, NCH-H, $J = 15.6$ Hz); 4.58 (d, 1H, NCH-H, $J = 15.6$ Hz); 7.30–7.40 (m, 4H, Ar); 8.19 (exch br s, 1H, NH). $^{13}$C-NMR (CDCl$_3$) $\delta$ 15.7 (CH$_3$); 21.1 (CH$_3$); 31.9 (CH); 34.1 (CH$_2$); 53.1 (CH$_2$); 116.8 (C); 121.4 (2 CH); 131.8 (2 CH); 136.8 (C); 158.6 (C); 166.3 (C); 166.5 (C). Anal. Calcd for C$_{14}$H$_{16}$BrN$_3$O$_2$ (338.20): C, 49.72; H, 4.77; N, 12.42; Found: C, 49.59; H, 4.75; N, 12.47.

### (±)N-(4-bromophenyl)-2-[3-methyl-6-oxo-4-phenyl-5,6-dihydropyridazin-1(4H)-yl]Acetamide, (±)6b

Yield = 62%; oil. $^1$H-NMR (CDCl$_3$) $\delta$ 2.06 (s, 3H, CH$_3$); 2.82 (dd, 1H, CHCH-H, $J = 4.8$ Hz, $J = 11.6$ Hz); 2.96 (dd, 1H, CHCH-H, $J = 7.6$ Hz, $J = 9.2$ Hz); 3.84 (dd, 1H, *CH*-Ph, $J = 5.2$ Hz, $J = 2.0$ Hz); 4.46 (d, 1H, NCH-H, $J = 15.6$ Hz); 4.72 (d, 1H, NCH-H, $J = 15.6$ Hz); 7.17–7.19 (m, 2H, Ar); 7.28–7.34 (m, 3H, Ar); 7.42 (d, 2H, Ar, $J = 8.8$ Hz) 7.90 (exch br s, 1H, NH). $^{13}$C-NMR (CDCl$_3$) $\delta$ 22.3 (CH$_3$); 34.4 (CH$_2$); 43.5 (CH); 53.7 (CH$_2$); 116.9 (C); 121.4 (CH); 127.2 (2 CH); 128.1 (CH); 129.2 (CH); 129.5 (2 CH); 131.8 (2 CH); 136.6 (C); 137.1 (C); 155.9 (C); 165.8 (C); 166.4 (C). Anal. Calcd for C$_{19}$H$_{19}$BrN$_3$O$_2$ (400.27): C, 57.01; H, 4.53; N, 10.50; Found: C, 57.17; H, 4.52; N, 10.47.

### N-(4-bromophenyl)-2-[3,4-dimethyl-6-oxopyridazin-1(6H)-yl]Acetamide, 7a

Yield = 81%; mp = 205–206°C (EtOH). $^1$H-NMR (CDCl$_3$) $\delta$ 2.23 (s, 3H, N = C*CH$_3$*); 2.33 (s, 3H, =C*CH$_3$*); 4.92 (s, 2H, CH$_2$); 6.81 (s, 1H, Ar); 7.39–7.44 (m, 4H, Ar); 9.11 (exch br s, 1H, NH). $^{13}$C-NMR (CDCl$_3$) $\delta$ 19.0 (CH$_3$); 19.2 (CH$_3$); 57.5 (CH$_2$); 116.0 (C); 121.0 (2CH); 127.4 (CH); 132.0 (2CH); 137.0 (C); 144.8 (C); 161.1 (C); 165.4 (C). Anal. Calcd for C$_{14}$H$_{14}$BrN$_3$O$_2$ (336.18): C, 50.02; H, 4.20; N, 12.50; Found: C, 50.16; H, 4.19; N, 12.53.

### N-(4-bromophenyl)-2-[3-methyl-6-oxo-4-phenylpyridazin-1(6H)-yl]Acetamide, 7b

Yield = 64%; mp = 199–200°C (EtOH). $^1$H-NMR (CDCl$_3$) $\delta$ 2.30 (s, 3H, CH$_3$); 5.01 (s, 2H, CH$_2$); 6.91 (s, 1H, Ar); 7.40–7.42 (m, 2H, Ar); 7.43–7.48 (m, 4H, Ar); 7.49–7.5 (m, 3H, Ar); 9.22 (exch br s, 1H, NH). $^{13}$C-NMR (CDCl$_3$) $\delta$ 20.4 (CH$_3$); 58.0 (CH$_2$); 116.9 (C); 121.4 (CH); 127.9 (CH); 128.0 (2CH); 128.9 (2CH); 129.4 (2CH); 131.8 (2CH); 135.5 (C); 137.0 (C); 145.5 (C); 148.3 (C); 161.0 (C); 165.2 (C). Anal. Calcd for C$_{19}$H$_{16}$BrN$_3$O$_2$ (398.25): C, 57.30; H, 4.05; N, 10.55; Found: C, 57.43; H, 4.06; N, 10.58.

### General Procedures for 9a-h

Compounds 9a-h were obtained starting from appropriate substrate of type 8 [Isomura et al., 1988; Pihlaja et al., 2002; Wang et al., 2005; Yarligan et al., 2005; Zhao et al., 2013] following the same procedure described for 4a-f. The final compounds were purified by column chromatography using cyclohexane/ethyl acetate 1:1 (for 9a,f,g), cyclohexane/ethyl acetate 1:2 (for 9b), cyclohexane/ethyl acetate 2:1 (for 9d), and CH$_2$Cl$_2$/CH$_3$OH 98:2 (9c,e) as eluents.

### 2-(5-acetyl-4-methyl-2-oxo-thiazol-3-yl)-N-(4-bromophenyl)Acetamide, 9a

Yield = 19%; mp = 228–230°C (EtOH). $^1$H-NMR (CDCl$_3$) $\delta$ 2.39 (s, 3H, CO*CH$_3$*); 2.65 (s, 3H, CH$_3$); 4.55 (s, 2H, CH$_2$CO); 7.34–7.44 (m, 4H, Ar); 8.19 (exch br s, 1H, NH). Anal. Calcd for C$_{14}$H$_{13}$BrN$_2$O$_3$S (369.23): C, 45.54; H, 3.55; N, 7.59; Found: C, 45.65; H, 3.54; N, 7.60.

### N-(4-bromophenyl)-2-(4-methyl-2-oxo-thiazol-3-yl)Acetamide, 9b

Yield = 35%; mp = 204–205°C (EtOH). $^1$H-NMR (CDCl$_3$) $\delta$ 2.40 (s, 3H, CH$_3$); 4.45 (s, 2H, CH$_2$CO); 5.85 (s, 1H, H5-thiazole); 7.36–7.43 (m, 4H, Ar); 8.43 (exch br s, 1H, NH). Anal. Calcd for

$C_{12}H_{11}BrN_2O_2S$ (327.20): C, 44.05; H, 3.39; N, 8.56; Found: C, 44.17; H, 3.39; N, 8.54.

### N-(4-bromophenyl)-2-(2-oxo-4-phenyl-thiazol-3-yl)Acetamide, 9c

Yield = 18%;   mp = 181–183°C   (EtOH).   $^1$H-NMR (CDCl$_3$) $\delta$ 4.41 (s, 2H, CH$_2$CO); 6.14 (s, 1H, H5-thiazole); 7.32 (s, 4H, Ar); 7.45 (s, 5H, Ar); 8.45 (exch br s, 1H, NH). $^{13}$C-NMR (CDCl$_3$) $\delta$ 48.8 (CH$_2$); 99.4 (CH); 117.1 (C); 121.3 (CH); 121.4 (CH); 129.9 (CH); 130.3 (CH); 130.8 (C); 131.8 (CH); 136.6 (C); 138.3 (C); 165.1 (2 CO). Anal. Calcd for $C_{17}H_{13}BrN_2O_2S$ (389.27): C, 52.45; H, 3.37; N, 7.20; Found: C, 52.29; H, 3.36; N, 7.22.

### N-(4-bromophenyl)-2-[4-(3-methoxyphenyl)-2-oxothiazol-3-yl]-Acetamide, 9d

Yield = 25%;   mp = 162–165°C   (EtOH).   $^1$H-NMR (CDCl$_3$) $\delta$ 3.83 (s, 3H, CH$_3$); 4.39 (s, 2H, CH$_2$CO); 6.15 (s, 1H, H5-thiazole); 7.01 (s, 3H, Ar); 7.42 (s, 5H, Ar); 8.63 (exch br s, 1H, NH). $^{13}$C-NMR (CDCl$_3$) $\delta$ 48.8 (CH$_2$); 55.5 (CH$_3$); 99.3 (CH); 114.3 (CH); 116.0 (CH); 116.9 (CH); 121.2 (CH); 121.4 (CH); 130.2 (CH); 131.5 (C); 131.7 (CH); 136.7 (C); 138.3 (C); 159.9 (C); 165.2 (CO); 174.2 (CO). Anal. Calcd for $C_{18}H_{15}BrN_2O_3S$ (419.29): C, 51.56; H, 3.61; N, 6.68; Found: C, 51.43; H, 3.60; N, 6.72.

### N-(4-bromophenyl)-2-[4-(4-methoxyphenyl)-2-oxothiazol-3-yl]Acetamide, 9e

Yield = 15%;   mp = 210–213°C   (EtOH).   $^1$H-NMR (CDCl$_3$) $\delta$ 3.84 (s, 3H, CH$_3$); 4.37 (s, 2H, CH$_2$CO); 6.07 (s, 1H, H5-thiazole); 6.96 (d, 2H, Ar, J = 8.8 Hz); 7.38 (m, 6H, Ar); 8.79 (exch br s, 1H, NH). $^{13}$C-NMR (CDCl$_3$) $\delta$ 48.7 (CH$_2$); 55.3 (CH$_3$); 100.1 (CH); 114.4 (CH); 115.8 (CH); 117.1 (CH); 121.7 (CH); 121.3 (CH); 129.8 (CH); 131.2 (C); 132.1 (CH); 135.9 (C); 138.4 (C); 160.1 (C); 164.2 (CO); 173. (CO). Anal. Calcd for $C_{18}H_{15}BrN_2O_3S$ (419.29): C, 51.56; H, 3.61; N, 6.68; Found: C, 51.61; H, 3.61; N, 6.65.

### N-(4-bromophenyl)-2-[4-(3-chlorophenyl)-2-oxothiazol-3-yl]Acetamide, 9f

Yield = 16%;   mp = 203–204°C   (EtOH).   $^1$H-NMR (CDCl$_3$) $\delta$ 4.37 (s, 2H, CH$_2$CO); 6.18 (s, 1H, H5-thiazole); 7.36–7.46 (m, 8H, Ar); 8.59 (exch br s, 1H, NH). Anal. Calcd for $C_{17}H_{12}BrClN_2O_2S$ (423.71): C, 48.19; H, 2.85; N, 6.61; Found: C, 48.35; H, 2.84; N, 6.62.

### N-(4-bromophenyl)-2-[4-(4-chlorophenyl)-2-oxothiazol-3-yl]Acetamide, 9g

Yield = 18%;   mp = 230–232°C   (EtOH).   $^1$H-NMR (CDCl$_3$) $\delta$ 4.36 (s, 2H, CH$_2$CO); 6.14 (s, 1H, H5-thiazole); 7.37–7.45 (m, 8H, Ar); 8.73 (exch br s, 1H, NH). Anal. Calcd for $C_{17}H_{12}BrClN_2O_2S$ (423.71): C, 48.19; H, 2.85; N, 6.61; Found: C, 48.03; H, 2.85; N, 6.63.

### N-(4-bromophenyl)-2-[4-(4-nitrophenyl)-2-oxothiazol-3-yl]Acetamide, 9h

Yield = 21%;   mp = 162–164°C   (EtOH).   $^1$H-NMR (CDCl$_3$) $\delta$ 4.38 (s, 2H, CH$_2$CO); 6.30 (s, 1H, H5-thiazole); 7.41 (s, 4H, Ar); 7.72 (d, 2H, Ar, J = 8.8 Hz); 8.83 (d, 2H, Ar, J = 8.8); 8.68 (exch br s, 1H, NH). Anal. Calcd for $C_{17}H_{12}BrN_3O_4S$ (434.26): C, 47.02; H, 2.79; N, 9.68; Found: C, 47.16; H, 2.78; N, 9.71.
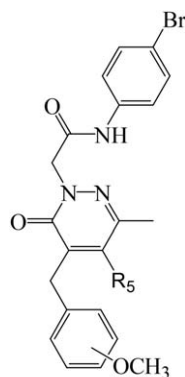
### 2-[4-(4-Aminophenyl)-2-Oxothiazol-3-Yl]-N-(4-bromophenyl)Acetamide, 10

Compound **9h** (0.11 mmol) was subject to catalytic reduction with 10% Pd/C (0.05 mmol) in EtOH (20 mL) for 2 h in a Parr instrument (30 PSI). The catalyst was filtered off, and the solvent was evaporated under vacuum, affording the final compound, which was purified by column chromatography using cyclohexane/ethyl acetate 1:1 as eluent. Yield = 27%; mp = 188–189°C (EtOH). $^1$H-NMR (CDCl$_3$) $\delta$ 4.32 (s, 2H, CH$_2$CO); 5.41 (exch br s, 2H, NH$_2$); 6.21 (s, 1H, H5-thyazole); 6.53 (m, 2H, Ar); 7.01 (m, 2H, Ar); 7.45 (s, 4H, Ar); 10.28 (exch br s, 1H, NH). Anal. Calcd for $C_{17}H_{14}BrN_3O_2S$ (404.28): C, 50.50; H, 3.49; N, 10.39; Found: C, 50.61; H, 3.48; N, 10.37.

### Cell Culture

Human promyelocytic leukemia HL60 cells stably transfected with FPR1 (FPR1-HL60), FPR2 (FPR2-HL60), or FPR3 (FPR3-HL60) were cultured in RPMI 1640 medium supplemented with 10% heat-inactivated fetal calf serum, 10 mM HEPES, 100 $\mu$g/ml streptomycin, 100 U/ml penicillin, and G418 (1 mg/mL), as previously described [Giovannoni et al., 2013]. Rat basophilic leukemia (RBL-2H3) cells transfected with mouse Fpr1 (Fpr1-RBL) or mouse Fpr2 (Fpr2-RBL) were cultured in DMEM supplemented with 20% (v/v) fetal bovine serum (FBS), 10 mM HEPES, 100 $\mu$g/ml streptomycin, 100 U/ml penicillin, and G418 (250 $\mu$g/ml). Wild-type HL60 and RBL-2H3 cells were cultured under the same conditions, but without G418.

**TABLE 1. Activity of 4-Benzyl-5-Substituted Pyridazinones 4a-f in Human Neutrophils and FPR-Transfected HL60 Cell**



4a-f

| | | | Ca$^{2+}$ flux | | | |
|---|---|---|---|---|---|---|
| | | | Human neutrophils | FPR1-HL60 | FPR2-HL60 | FPR3-HL60 |
| Compd | R$_5$ | OCH$_3$ | EC$_{50}$ (µM) and efficacy (%)[a] | | | |
| 4a | CH$_3$ | m | 0.006 ± 0.002 (150) | 0.019 ± 0.005 (85) | 0.043 ± 0.016 (80) | 0.040 ± 0.011 (165) |
| 4b | CH$_3$ | p | 0.27 ± 0.025 (140) | 0.9 ± 0.033 (60) | 0.013 ± 0.003 (95) | 0.13 ± 0.032 (100) |
| 4c | C$_2$H$_5$ | m | 1.2 ± 0.3 (100) | 3.2 ± 0.6 (120) | 1.9 ± 0.41 (100) | 4.1 ± 1.7 (100) |
| 4d | C$_3$H$_5$ | m | 3.2 ± 1.2 (70) | 2.2 ± 0.5 (115) | 4.6 ± 1.3 (90) | 3.4 ± 0.76 (65) |
| 4e | C$_4$H$_9$ | m | 2.7 ± 0.7 (25) | N.A.[b] | 15.7 ± 4.2 (90) | N.A. |
| 4f | C$_6$H$_5$ | m | 5.4 ± 0.26 (100) | 2.2 ± 0.62 (160) | N.A. | N.A. |

[a]EC$_{50}$ values represent the average of means from three independent experiments and were determined by nonlinear regression analysis of the concentration-response curves (5–6 points) generated using GraphPad Prism 5 with 95% confidential interval ($P < 0.05$). Efficacy is expressed as % of the response induced by 5 nM fMLF (FPR1), 5 nM WKYMVm (FPR2), or 10 nM WKYMVM (FPR3).
[b]N.A., no activity (no response was observed during the first 2 min after addition of compounds under investigation) considering the limits of efficacy > 20% and EC$_{50}$ < 50 µM.
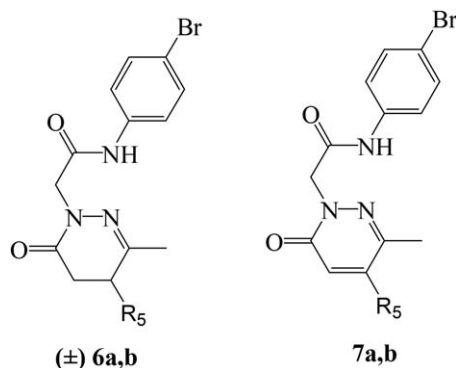
## Isolation of Human Neutrophils

Blood was collected from healthy donors in accordance with a protocol approved by the Institutional Review Board at Montana State University. Neutrophils were purified from the blood using dextran sedimentation, followed by Histopaque 1077 gradient separation and hypotonic lysis of red blood cells, as previously described [Schepetkin et al., 2014b]. Isolated neutrophils were washed twice and resuspended in HBSS without Ca$^{2+}$ and Mg$^{2+}$ (HBSS$^-$). Neutrophil preparations were routinely > 95% pure, as determined by light microscopy, and greater than 98% viable, as determined by trypan blue exclusion.

## Isolation of Murine Neutrophils

Murine bone marrow neutrophils were isolated from bone marrow leukocyte preparations, as described previously [Schepetkin et al., 2014a].

Briefly, bone marrow leukocytes were flushed from tibias and femurs of BALB/c mice with HBSS, filtered through a 70 µm nylon cell strainer (BD Biosciences, Franklin Lakes, NJ) to remove cell clumps and bone particles, and resuspended in HBSS at 10$^6$ cells/ml. Bone marrow leukocytes were resuspended in 3 ml of 45% Percoll solution and layered on top of a Percoll gradient consisting of 2 ml each of 50, 55, 62, and 81% Percoll solutions in a conical 15-ml polypropylene tube. The gradient was centrifuged at 1600g for 30 min at 10°C, and the cell band located between the 61 and 81% Percoll layers was collected. The cells were washed, layered on top of 3 ml of Histopaque 1119, and centrifuged at 1600g for 30 min at 10°C to remove contaminating red blood cells. The purified neutrophils were collected, washed, and resuspended in HBSS. All animal use was conducted in accordance with a protocol approved by the Institutional Animal Care and Use Committee at Montana State University.

**TABLE 2. Activity of C-5 Substituted Pyridazinones (±)−6a-b and 7a-b in Human Neutrophils and FPR-Transfected HL60 Cells**



(±) 6a,b          7a,b

| | | Ca$^{2+}$ flux | | | |
|---|---|---|---|---|---|
| | | Human neutrophils | FPR1-HL60 | FPR2-HL60 | FPR3-HL60 |
| Compd | R$_5$ | EC$_{50}$ (µM) and efficacy (%)[a] | | | |
| (±)-6a | CH$_3$ | 13.0 ± 1.8 (115) | 13.0 ± 4.6 (60) | 2.6 ± 0.89 (120) | 11.8 ± 3.0 (150) |
| (±)-6b | C$_6$H$_5$ | 1.4 ± 0.38 (75) | 4.1 ± 1.6 (90) | 0.63 ± 0.17 (110) | 0.49 ± 0.14 (120) |
| 7a | CH$_3$ | 2.0 ± 0.29 (130) | 5.7 ± 2.1 (110) | 0.51 ± 0.19 (90) | N.A.[b] |
| 7b | C$_6$H$_5$ | 0.20 ± 0.056 (110) | N.A. | 0.15 ± 0.052 (115) | 0.97 ± 0.23 (95) |

[a]EC$_{50}$ values represent the average of means from three independent experiments and were determined by nonlinear regression analysis of the concentration-response curves (5–6 points) generated using GraphPad Prism 5 with 95% confidential interval ($P < 0.05$). Efficacy is expressed as % of the response induced by 5 nM fMLF (FPR1-HL60), 5 nM WKYMVm (FPR2-HL60), or 10 nM WKYMVM (FPR3-HL60).
[b]N.A., no activity (no response was observed during first 2 min after addition of compounds under investigation) considering the limits of efficacy > 20% and EC$_{50}$ < 50 µM.
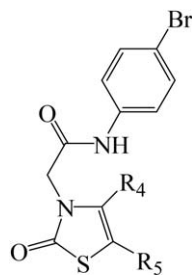
## Ca$^{2+}$ Mobilization Assay

Changes in intracellular Ca$^{2+}$ were measured with a FlexStation II scanning fluorometer using a FLIPR 3 calcium assay kit (Molecular Devices, Sunnyvale, CA) for human and murine neutrophils, as well as HL60 and RBL cells, as described previously [Schepetkin et al., 2013]. All active compounds were evaluated in wild-type HL60 and RBL cells to verify that the agonists are inactive in non-transfected cells. Neutrophils or HL60 and RBL cells, suspended in HBSS$^-$ containing 10 mM HEPES, were loaded with Fluo-4 AM dye (Invitrogen; 1.25 µg/mL final concentration) and incubated for 30 min in the dark at 37°C. After dye loading, the cells were washed with HBSS$^-$ containing 10 mM HEPES, resuspended in HBSS containing 10 mM HEPES and Ca$^{2+}$ and Mg$^{2+}$ (HBSS$^+$), and aliquotted into the wells of a flat-bottomed, half-area-well black microtiter plates (2 × 10$^5$ cells/well). The compound of interest was added from a source plate containing dilutions of test compounds in HBSS$^+$, and changes in fluorescence were monitored ($\lambda_{ex} = 485$ nm, $\lambda_{em} = 538$ nm) every 5 s for 240 s at room temperature after automated addition of compounds. Maximum change in fluorescence, expressed in arbitrary units over baseline, was used to determine agonist response. Responses were normalized to the response induced by 5 nM fMLF (Sigma Chemical Co., St. Louis, MO) for FPR1 HL60 cells and human neutrophils, 5 nM WKYMVm (Calbiochem, San Diego, CA) for FPR2 HL60 cells, 10 nM WKYMVM (Tocris Bioscience) for FPR3-HL60 cells, and 10 nM WKYMVm for mouse neutrophils, mFpr1-RBL, and mFpr2-RBL cells, which were assigned a value of 100%. Curve fitting (5–6 points) and calculation of median effective concentration values (EC$_{50}$ values) were performed using nonlinear regression analysis of the concentration-response curves generated using Prism 5 (GraphPad Software, Inc., San Diego, CA).

## Cell Migration Assay

Neutrophils were suspended in HBSS$^+$ containing 2% (v/v) FBS (2 × 10$^6$ cells/mL), and cell migration was analyzed in 96-well ChemoTx chemotaxis chambers (Neuroprobe, Gaithersburg, MD), as previously described [Schepetkin et al., 2014b]. Briefly,

**TABLE 3. Activity of 9a-h, 10 in Human Neutrophils and FPR-Transfected HL60 Cells**



**9a-h, 10**

| | | | Ca$^{2+}$ flux | | | |
|---|---|---|---|---|---|---|
| | | | Human neutrophils | FPR1-HL60 | FPR2-HL60 | FPR3-HL60 |
| Compd | R$_4$ | R$_5$ | EC$_{50}$ (μM) and efficacy (%)[a] | | | |
| 9a | CH$_3$ | COCH$_3$ | 12.2 ± 2.5(55) | 8.9 ± 1.9 (75) | 5.8 ± 1.4 (60) | N.A.[b] |
| 9b | CH$_3$ | H | 10.7 ± 2.3 (55) | 12.4 ± 2.6 (70) | 4.1 ± 1.1 (80) | 27.8 ± 3.2 (85) |
| 9c | Ph | H | 6.0 ± 1.5 (95) | 1.8 ± 0.6 (100) | 2.1 ± 0.6 (95) | 19.7 ± 2.4 (135) |
| 9d | 3-OCH$_3$Ph | H | 1.3 ± 0.3 (125) | 0.28 ± 0.08 (90) | 0.23 ± 0.04 (120) | 5.1 ± 1.7 (100) |
| 9e | 4-OCH$_3$Ph | H | 7.4 ± 2.3 (110) | 2.6 ± 0.6 (110) | 1.8 ± 0.16 (100) | 36.1 ± 3.3 (85) |
| 9f | 3-ClPh | H | 11.1 ± 2.8 (140) | 6.0 ± 1.7 (75) | 3.0 ± 0.7 (110) | 32.2 ± 3.6 (75) |
| 9g | 4-ClPh | H | 12.2 ± 3.1 (125) | 2.8 ± 0.7 (75) | 2.4 ± 0.5 (75) | N.A. |
| 9h | 4-NO$_2$Ph | H | 1.5 ± 0.4 (95) | 9.1 ± 1.4 (60) | N.A. | N.A. |
| 10 | 4-NH$_2$Ph | H | 36.1 ± 3.9 (65) | 34.9 ± 4.2 (80) | 14.7 ± 3.7 (65) | N.A. |

[a]EC$_{50}$ values represent the average of means from three independent experiments and were determined by nonlinear regression analysis of the concentration-response curves (5–6 points) generated using GraphPad Prism 5 with 95% confidential interval ($P < 0.05$). Efficacy is expressed as % of the response induced by 5 nM fMLF (FPR1-HL60), 5 nM WKYMVm (FPR2-HL60), or 10 nM WKYMVM (FPR3-HL60).
[b]N.A., no activity (no response was observed during first 2 min after addition of compounds under investigation) considering the limits of efficacy > 20% and EC$_{50}$ < 50 μM.

**TABLE 4. Chemoattractant Activity of Selected Pyridazinones in Human Neutrophils**

| Compd | EC$_{50}$ (μM)[a] |
|---|---|
| 4a | 0.27 ± 0.06 |
| 4b | 0.51 ± 0.11 |
| 7b | 2.1 ± 0.53 |

[a]The data are presented as the mean ± SD of three independent experiments with cells from different donors, in which median effective concentration values (EC$_{50}$) were determined by nonlinear regression analysis of the concentration-response curves (5–6 points) generated using GraphPad Prism 5 with 95% confidential interval ($P < 0.05$).

lower wells were loaded with 30 μL of HBSS$^+$ containing 2% (v/v) FBS and the indicated concentrations of test compound, DMSO (negative control), or 1 nM fMLF as a positive control. Neutrophils were added to the upper wells and allowed to migrate through the 5.0 μm pore polycarbonate membrane filter for 60 min at 37°C and 5% CO$_2$. The number of migrated cells was determined by measuring ATP in lysates of transmigrated cells using a luminescence-based assay (CellTiter-Glo; Promega, Madison, WI), and luminescence measurements were converted to absolute cell numbers by comparison of the values with standard curves obtained with known numbers of neutrophils. The results are expressed as percentage of negative control and were calculated as follows: (number of cells migrating in response to test compounds/spontaneous migration in response to control medium)×100. EC$_{50}$ values were determined by nonlinear regression analysis of the concentration-response curves generated using Prism 5 software.

## RESULTS AND DISCUSSION

The newly synthesized compounds were evaluated for their ability to induce intracellular Ca$^{2+}$ flux in human neutrophils and HL60 cells transfected with FPR1, FPR2, and FPR3 (Tables 1–3). Compounds were also evaluated in mouse neutrophils and RBL-2H3 cells transfected with mouse FPR1 and FPR2. To verify receptor specificity, these compounds were also evaluated, as applicable, in wild-type non-transfected HL60 and RBL cells and were found to be inactive.

**TABLE 5. Activity of Selected Pyridazinones in Mouse Neutrophils and Mouse Fpr-Transfected RBL Cells**

|  | $Ca^{2+}$ flux | | |
| --- | --- | --- | --- |
|  | Mouse neutrophils | mFpr1-RBL | mFpr2-RBL |
| Compd | $EC_{50}$ (μM) and efficacy (%)[a] | | |
| **4a** | N.A.[b] | N.A. | N.A. |
| **4b** | N.A. | N.A. | N.A. |
| **4f** | 24.3 ± 4.8 (95) | N.A. | 28.8 ± 5.2 (180) |
| **(±)-6a** | N.A. | 25.1 ± 4.5 (70) | N.A |
| **(±)-6b** | 14.2 ± 3.4 (160) | 2.3 ± 0.7 (60) | 3.5 ± 1.1 (220) |
| **7a** | 21.7 ± 5.2 (70) | N.A. | N.A. |
| **7b** | 15.7 ± 4.1 (75) | N.A. | N.A |

[a]$EC_{50}$ values represent the average of means from three independent experiments and were determined by nonlinear regression analysis of the concentration-response curves (5–6 points) generated using GraphPad Prism 5 with 95% confidential interval ($P < 0.05$). Efficacy is expressed as % of the response induced by 10 nM WKYMVm.
[b]N.A., no activity (no response was observed during first 2 min after addition of the compounds under investigation).

In the 4-benzylpyridazinone series (Table 1), the introduction of a methyl at C-5 was associated with high FPR agonist activity (compounds **4a,b**) leading to some of themost potent mixed agonists. For example, **4a** activated all three FPR subtypes with good potency (FPR1 $EC_{50} = 19$ nM, FPR2 $EC_{50} = 43$ nM, FPR3 $EC_{50} = 40$ nM). Although **4b** was an FPR1 and FPR3 agonist with submicromolar activity ($EC_{50} = 0.9$ and 0.13 μM, respectively), it exhibited a preference for FPR2 ($EC_{50} = 13$ nM).These results are consistent with our previous studies [Cilibrizzi et al., 2009], which showed that when $OCH_3$ was shifted from the *meta* to the *para* position of the benzyl at C-4, the selectivity of a given ligand shifted from mixed FPR1/FPR2 to FPR2-specific.

Elongation of the aliphatic chain (compounds **4c-e**) was detrimental for activity and led to mixed agonists with $EC_{50}$ values in the micromolar range, with the exception of the 3-butyl derivative **4e**, which was a weak but selective FPR2 agonist ($EC_{50} = 15.7$ μM). Surprisingly, the 5-phenyl derivative **4f** exhibited FPR1 selectivity ($EC_{50} = 2.2$ μM, Table 1).

As shown in Table 2 elimination of the substituent at position 4 and introduction of $CH_3$ or $C_6H_5$ at C-5 (products of type **6** and **7**) led to compounds endowed with micromolar activity and a slight preference for FPR2. The unsaturation at C-4/C-5 of the heterocyclic ring (**7a,b**) appeared to be associated with increased agonist activity and selectivity (generally submicromolar range) relative to the 4,5-dihydro analogues, **(±)6a,b**. As compounds **(±)6a,b** were

mixtures of isomers, it is possible that one of the isomers could be more active than the other, reducing overall specific activity or even interfering with binding of the active isomer.

Table 3 reports the activities of the 2-oxothiazole derivatives, **9a-h** and **10** that exhibited $EC_{50}$ values in the micromolar range for the three FPR isoforms, with the exception of compound **9d**, which had $EC_{50}$ values of 0.28 μM and 0.23 μM for FPR1 and FPR2, respectively. No appreciable FPR2 selectivity was observed for this series, although they did have a lower affinity for FPR3 ($EC_{50} \sim 20$-fold higher than for FPR1 and FPR2).

The most active derivatives (**4a,b** and **7b**) were also evaluated for their chemoattractant activity toward human neutrophils (Table 4). As expected for FPR agonists, they stimulated neutrophil migrations with $EC_{50}$ values that correlated well with their ability to induce human neutrophil intracellular $Ca^{2+}$ flux.

All of the synthesized compounds were also evaluated in mouse neutrophils and RBL cells transfected with mouse Fpr1 or Fpr2 (Table 5). The majority of tested compounds had no agonist effects at mouse neutrophils or RBL cells transfected with mouse Fpr; however, four compounds were active in mouse neutrophils and three had activity in either Fpr1 or Fpr2 RBL cells. As shown in Table 5, compounds **4f**, **(±)6a,b**, and **7a,b** all activated $Ca^{2+}$ flux in mouse neutrophils with low micromolar activity. From the literature, it is well known that there are differences in affinity between FPR1 and Fpr1 for *f*MLF and other FPR agonists/antagonists [He et al., 2000] and these receptors have only 72% sequence similarities [Dahlgren et al., 2016]. However, it is difficult to explain the complete inactivity of the most potent human FPR agonists of this series (**4a** and **4b**) toward mouse neutrophils or mouse Fpr-transfected RBL cells. Comparison of the results between human FPR-transfected HL60 cells and mouse Fpr1/Fpr2-transfected RBL cells was also difficult to interpret. For example, **(±)6a** was active for all human FPR and mouse Fpr subtypes tested, whereas **4f** was inactive in FPR2-HL60 cells but had an $EC_{50}$ value of 28.8 μM for mouse Fpr2. Likewise, **(±)6a** was active for all human FPR subtypes but only activated mFpr1 and not mouse neutrophils or mFpr2. Thus, the difference in human and mouse FPR responses to various agonists are clearly evident and will need to be considered when using agonists in mouse models involving Fpr function.

In conclusion, we have identified a new series of FPRs agonists with $EC_{50}$ values in the nanomolar to low micromolar range. The majority of compounds were mixed FPRs agonists, but with a slight

preference for FPR2. Compounds **4a** and **4b** are notable for their high potency. In particular, compound **4a** is a mixed FPR agonist with $EC_{50}$ values of 19 nM (FPR1), 43 nM (FPR2), and 40 nM (FPR3). Similarly interesting is compound **4b**, which had considerable potency, but exhibited a preference for FPR2 ($EC_{50} = 13$ nM) and could represent a novel lead compound for further chemical manipulation and studies.

## REFERENCES

Beutler B. 2004. Innate immunity: an overview. Mol Immunol 40: 845–859.

Bozinovski S, Anthony D, Anderson GA, Irving LB, Levy BD, Vlahos R. 2013. Treating neutrophilic inflammation in COPD by treating ALX/FPR2 resolution pathways. Pharmacol Ther 140:280–289.

Cilibrizzi A, Crocetti L, Giovannoni MP, Graziano A, Vergelli C, Bartolucci G, Soldani G, Quinn MT, Schepetkin IA, Faggi C. 2013. Synthesis, HPLC enantioresolutio and X-ray analysis of a new series of C5-methyl pyridazines as N-formyl peptide receptor (FPR) agonists. Chirality 25:400–408.

Cilibrizzi A, Quinn MT, Kirpotina LN, Schepetkin IA, Holderness J, Ye RD, Rabiet MJ, Biancalani C, Cesari N, Graziano A, et al. 2009. 6-Methyl-2,4-disubstituted pyridazin-3(2H)-ones: a novel class of small-molecule agonists for formyl peptide receptors. J Med Chem 52:5044–5057.

Cilibrizzi A, Schepetkin IA, Bartolucci G, Crocetti L, Dal Piaz V, Giovannoni MP, Graziano A, Kirpotina LN, Quinn MT, Vergelli C. 2012. Synthesis, enantioresolution, and activity profile of chiral 6-methyl-2,4-disubstituted pyridazin-3(2H)-ones as potent N-formyl peptide receptor agonists. Bioorg Med Chem 20:3781–3792.

Coates WJ, McKillop A. 1993. One-pot preparation of 6-substituted 3(2H)-pyridazinones from ketones. Synthesis 3: 334–342.

Corminboeuf O, Leroy X. 2015. FPR2/ALXR agonists and the resolution of inflammation. J Med Chem 58:537–559.

Crocetti L, Vergelli C, Cilibrizzi A, Graziano A, Khlebnikov AI, Kirpotina LN, Schepetkin IA, Quinn MT, Giovannoni MP. 2013. Synthesis and pharmacological evaluation of new pyridazin-based thioderivatives as formyl peptide receptor (FPR) agonists. Drug Dev Res 74:259–271.

Dahlgren C, Gabl M, Holdfeldt A, Winther M, Forsman H. 2016. Basic characteristics of the neutrophil receptors that recognize formylated peptides, a danger-associated molecular pattern generated by bacteria and mitochondria. Biochem Pharmacol 114:22–39.

Giovannoni MP, Schepetkin IA, Cilibrizzi A, Crocetti L, Khlebnikov AI, Dahlgren C, Graziano A, Dal Piaz V, Kirpotina LN, Zerbinati S, et al. 2013. Further studies on 2-arylacetamide pyridazin-3(2H)-ones: design, synthesis and evaluation of 4,6-disubstituted analogs as formyl peptide receptors (FPRs) agonists. Eur J Med Chem 64:512–528.

Haider N, Holzer W. 2004. Product class 8: pyridazines. Sci Synth 16:125–249.

He R, Tan L, Browning DD, Wang JM, Ye DR. 2000. The synthetic peptide Trp-Lys-Tyr-Met-Val-D-Met is a potent chemotactic agonist for mouse formyl peptide receptor. J Immunol 165:4598–4605.

Holloway CA, Muratore ME, Storer RI, Dixon DJ. 2010. Direct enantioselective bronsted acid catalyzed N-acyliminium cyclization cascades of tryptamines and ketoacids. Org Lett 12:4720–4723.

Isomura Y, Sakamoto S, Yoshida M, Abe T. 1988. Preparation of 4-aryl-2(3H)-thiazolone derivative as drug for bone disorders. Jpn Kokai Tokkyo Koho JP 63112574 (A)-1988-05-17.

Libby P. 2002. Atherosclerosis: the new view. Sci Am 286:46–52.

Libby P. 2015. Fanning the flames: inflammation in cardiovascular diseases. Cardiov Res 107:307–309.

Mantovani A, Allavena P, Sica A, Balkwill F. 2008. Cancer-related inflammation. Nature 454:436–444.

Metz G, Schwenker G. 1980. Intramolecular cyclocondensation of 4- and 5-oxocarboxylic acids to five a membered ring systems. Synthesis 5:394–397.

Migeotte I, Communi D, Parmentier M. 2006. Formyl peptide receptors: a promiscuous sub family of G protein-coupled receptors controlling immune responses. Cytokine Grow Factor Rev 17:501–519.

Migeotte I, Riboldi E, Franssen JD, Gregoire F, Loison C, Wittamer V, Detheux M, Robberecht P, Costagliola S, Vassart G, et al. 2005. Identification and characterization of an endogenous chemotactic ligand specific for FPRL2. J Exp Med 201: 83–93.

Pihlaja K, Ovcharenko V, Kohlemainen E, Laihia K, Fabian Walter MF, Dehne H, Perjessy A, Kleist M, Teller J, Šustekovà Z. 2002. A correlative IR, MS, $^{1}$H, $^{13}$C and $^{15}$N NMR and theoretical study of 4-arylthiazol-2(3H)-ones. J Chem Soc Perkin Trans 2:329–336.

Pinna GA, Curzu MM, Barlocco D, Cignarella G, Cavalletti E, Germini M, Berger K. 1988. Synthesis and pharmacological study of 5-aryl-6-methyl-4,5-dihydropyridazin-3(2H)-ones and related 5-aryl-6-methylpyridazin-3(2H)-ones. Farmaco 43:539–549.

Serhan CN, Chiang N, Dalli J. 2015. The resolution code of acute inflammation: novel pro-resolving lipid mediators in resolution. Semin Immunol 27:200–215.

Serhan CN, Hong S, Gronert K, Colgan SP, Devchand PR, Mirick G, Moussignac RL. 2002. Resolvins: a family of bioactive products of omega-3 fatty acid transformation circuits initiated by aspirin treatment that counter pro-inflammation signals. J Exp Med 196:1025–1037.

Serhan CN, Krishnamoorthy S, Recchiuti A, Chiang N. 2011. Novel anti-inflammatory-pro-resolving mediators and their receptors. Curr Top Med Chem 11:629–647.

Serhan CN, Levy B. 2003. Novel pathways and endogenous mediators in anti-inflammation and resolution. Chem Immunol Allergy 83:115–145.

Schepetkin AI, Khlebnikov AI, Giovannoni MP, Kirpotina LN, Cilibrizzi A, Quinn MT. 2014a. Development of small molecule non-peptide formyl peptide receptor (FPR) ligands and molecular modeling of their recognition. Curr Med Chem 21:1478–1504.

Schepetkin AI, Kirpotina LN, Khlebnikov AI, Leopoldo M, Lucente E, Lacivita E, De Giorgio P, Quinn MT. 2013. 3-(1H-indol-3-yl)-2-[3-(4-nitrophenyl)ureido]propanamide enantiomers with human formyl-peptide receptor agonist activity: molecular

modeling of chiral recognition by FPR2. Biochem. Pharmacol 85:404–416.

Schepetkin IA, Kirpotina LN, Khlebnikov AI, Cheng N, Ye RD, Quinn MT. 2014b. Antagonism of human formyl peptide receptor 1 (FPR1) by chromones and related isoflavones. Biochem Pharmacol 92:627–641.

Vergelli C, Schepetkin IA, Ciciani G, Cilibrizzi A, Crocetti L, Giovannoni MP, Guerrini G, Iacovone A, Kirpotina LN, Khlebnikov AI, et al. 2016. 2-Arylacetamido-4-phenylamino-5-substituted pyridazinones as formyl peptide receptors agonists. Bioorg Med Chem 24:2530–2543.

Wang S, Wood G, Duncan KW, Meades C, Gibson D, McLachlan JC, Perry A, Blake D, Zheleva DI, Fisher P. 2005. Preparation of pyrimidinylthiazolone compounds as protein kinase inhibitors. PCT Int Appl WO 2005042525.

Xu Y, Han B, Xie L, Maynard G. 2005. Preparation of imidazopyridazines, triazolopyridazines and related benzodiazepine receptor ligands. PCT Int Appl WO2005080355(A1)-2005-09-01.

Yarligan S, Ogretir C, Csizmadia IG, Acikkalpe E, Bierber H, Arsian T. 2005. An ab initio study on protonation of some substituted thiazole derivates. J Mol Struct Theochem 715:199–203.

Ye RD, Boulay F, Wang JM, Dahlgren C, Gerard C, Parmentier M, Serhan CN, Murphy PM. 2009. International union of basic and clinical pharmacology. LXXIII. Nomenclature for the formyl peptide receptor (FPR) family. Pharmacol Rev 61:119–161.

Zhao L, Cao D, Chen T, Whang YMZ, Xu Y, Chen WWX, Lin Y, Du Z, Xiong B, Li J, et al. 2013. Fragment-based drug discovery of 2-thiazolidinones as inhibiors of the histone reader BRD4 bromodomain. J Med Chem 56:3833–3851.